

Mismatched Filter Design and Interference Mitigation for MIMO Radars

Tuomas Aittomäki, *Member, IEEE*, and Visa Koivunen, *Fellow, IEEE*

Abstract—MIMO radar receivers need to reliably separate waveforms originating from different transmitters while suppressing interference for effective operation. In order to achieve this goal, mismatched filters may be employed at the receivers. By using mismatched filters, it is possible to reduce the power of the interference while strictly controlling the autocorrelation sidelobe and peak cross-correlation levels of the received waveforms. In this paper, we propose a mismatched filter design method that minimizes interference and jamming power at the filter output while the peak sidelobe and cross-correlation levels for all Doppler frequencies are constrained to desired values. The proposed design method is formulated as an optimization problem employing sum-of-squares representation of nonnegative polynomials and solved using semidefinite relaxation. It is demonstrated that good interference suppression performance is achieved even when using an estimated covariance matrix.

Index Terms—MIMO radar, filter design, mismatched filter, interference suppression, jamming, convex optimization, semidefinite relaxation, polynomial constraints

I. INTRODUCTION

MIMO radar is a radar concept in which multiple transmitters transmit different waveforms simultaneously. The MIMO radar system can be either distributed or colocated. In the distributed MIMO radar, the transmitters and the receivers are spatially distributed over a wide area [1]. In the colocated case, the transmitters and receivers are at the same location, respectively [2].

We consider the filter design for receiving waveforms with slow-time coding [3]. Unlike for fast-time coding, the Doppler frequency cannot be typically assumed to be zero for waveforms using slow-time coding. Optimal operation of the MIMO radar requires that the waveforms can be separated at the receiver end, which would typically require that the transmitted waveforms are orthogonal. However, it is not possible to have waveforms that are orthogonal for all time delays and Doppler shifts [4]. It is nevertheless possible to improve the cross-correlation properties of the waveforms by using mismatched filters at the receiver. The mismatched filter design proposed in this paper can be applied to both colocated and distributed MIMO radar configurations as well as in conventional radars for sidelobe reduction and interference mitigation.

In order to obtain waveforms that would be as close to orthogonal as possible, optimization of transmitted waveforms

for MIMO radar has been studied in the past. Simulated annealing and iterative code selection were combined to search for orthogonal polyphase codes in [5]. Similar approach using genetic algorithm was used in [6]. Tabu search algorithm was used in [7] and the cross-entropy method in [8]. The Doppler effect was not considered in the optimization of the codes in any of these papers. In [6] and [8], the Doppler properties of the obtained codes was checked only for a zero delay. Despite numerous optimization approaches, the optimized transmit waveforms remain far from orthogonal. Consequently, optimization of also the receiver end is appealing.

Improving the orthogonality of the waveforms at the receiver is possible using mismatched filters [9]. In mismatched filtering, the received signal is correlated with a modified version of the transmitted waveform instead of an exact copy. It is known that the matched filter that correlates the transmitted waveform with itself maximizes the SNR in additive white Gaussian noise, but the peak autocorrelation sidelobe is fixed for a matched filter. Mismatched filters have been traditionally used in radars to reduce the sidelobes at the cost of a reduced SNR [9].

Previously, clutter rejection with mismatched filtering for binary sequences has been proposed in [10]. Mismatched filter with Pareto-optimal integrated sidelobe and the peak sidelobe levels was developed in [11]. Mismatched filterbank design for MIMO radars was considered in [12] for limiting the peak autocorrelation sidelobe and cross-correlation levels. Interference and jamming power was minimized in [13] while maintaining desired autocorrelation sidelobe and cross-correlation levels. However, Doppler shift was assumed to be zero in these studies. With slow-time coding, moving targets have nonzero Doppler frequencies. Hence, taking the Doppler shift into account is crucial as even a small Doppler shift can result in a large sidelobe in a otherwise good autocorrelation function.

A filter design method minimizing the integrated sidelobe level also for nonzero Doppler have been proposed in [14]. However, that method cannot constrain the peak sidelobe level for nonzero Doppler shifts. In this paper, we develop a mismatched filter design method that minimizes the interference and noise power at the filter output while maintaining desired peak sidelobe and cross-correlation levels over all Doppler frequencies.

The proposed filter design method is based on sum-of-squares representation of nonnegative polynomials. This allows for a conversion of the constraints with continuous Doppler frequency into positive-semidefinite (PSD) matrix constraints [15]. The sum-of-squares representation has been previously used in radar waveform design for optimizing the

Copyright (c) 2016 IEEE. Personal use of this material is permitted. However, permission to use this material for any other purposes must be obtained from the IEEE by sending a request to pubs-permissions@ieee.org

This work was supported by the Finnish Defence Research Agency.

T. Aittomäki and V. Koivunen are within Department of Signal Processing and Acoustics, Aalto University, PO Box 13000, FI-00076 Aalto, Finland, tuomas.aittomaki@aalto.fi, visa.koivunen@aalto.fi

worst case SNR with respect to the received Doppler [16]. However, it has not been used before to limit the peak sidelobe and cross-correlation levels.

In order to get a convex optimization problem, we also apply semidefinite relaxation (SDR) [17]. The solution of the SDR problem is a matrix from which the filter coefficients have to be extracted. If the solution is a rank-one matrix, factorization of the solution yields a filter vector that is a globally optimal solution of the original problem. Otherwise, randomization methods [17] can be used to find the actual filter coefficients. The drawback of the randomization is that even though the SNR loss can be scaled to desired value, the sidelobe and cross-correlation constraints cannot be guaranteed to be satisfied. However, as the generation of the approximate solutions is very simple, good results can be achieved by generating a large number of the randomized solutions, see [17] for further details on the randomization method.

As the computational complexity of the SDR problem can be high, we also propose a discretized filter design method that can be formulated as a convex quadratically constrained problem (QCP). Solutions to this problem can be found with significantly reduced computational complexity. It will be shown in the examples that a mismatched filter designed with the proposed method can provide a significant gain in SINR compared to the matched filter while maintaining the desired low sidelobe and cross-correlation levels.

The proposed method of minimizing the interference and noise power requires the interference plus noise covariance matrix to be known or reliably estimated. If there is no auxiliary channel for noise and interference measurements or if the transmitter cannot be turned off while the covariance matrix is estimated, the estimates will also contain a desired signal component. We formulate the filter optimization problem so that the signal loss within the Doppler bin can be constrained to a desired level. In the numerical examples, it is demonstrated that the amount of samples used in the filtering is also sufficient to estimate the covariance matrix for efficient interference suppression. Furthermore, it is possible to use regularized estimators [18], [19] of the covariance matrix when the sample support is small or the interference is non-Gaussian.

This paper is organized as follows: The basic principles of mismatched filter design are described in Section II. Section III introduces the proposed semidefinite relaxation of the mismatched filter design problem. This section also contains a brief introduction to sum-of-squares presentation of polynomials citing the results of [15]. The computational complexity of the SDR method is high, so in Section IV, we propose an approximate filter design method with reduced computational complexity. Section V contains a short discussion on making the trade-off between interference attenuation and the sidelobe and the cross-correlation levels. Numerical results are provided in Section VI. Finally, the concluding remarks are presented in Section VII.

II. FILTER DESIGN PRINCIPLE

The objective of the mismatched filter design proposed here is a filter that minimizes the output noise plus interference

power while maintaining unit gain for the signal of interest. We assume that the transmit waveforms are known at the receiver. The optimization of the filter coefficients of a MIMO radar system can be done centrally or in a distributed manner in each receiver.

A. Mismatched Filtering

We consider designing the filter coefficients for receiving one of the several transmitted waveforms. The process can then be repeated for all the employed MIMO radar waveforms to form a filterbank with multiple filters. The design method can be applied to both distributed and colocated MIMO radar configurations.

The filter that is to be designed has L coefficients. An $L \times 1$ vector containing these coefficients is denoted by \mathbf{w} . We assume that the waveforms consist of N symbols and that the symbols of the waveform number k are $\{s_{k,1}, s_{k,2}, \dots, s_{k,N}\}$. Define the n th element of a $L \times 1$ waveform vector as

$$(\mathbf{s}_k(m))_n = \begin{cases} s_{k,n+m}, & 1 \leq n+m \leq N \\ 0, & \text{otherwise} \end{cases} \quad (1)$$

where m is the propagation delay of the received waveform, so the vector $\mathbf{s}_k(m)$ contains some (or all) of the symbols depending on the delay. Without loss of generality, \mathbf{s}_k can be normalized such that

$$\|\mathbf{s}_k(0)\| = 1. \quad (2)$$

With the narrowband assumption, the received waveform can be written as [16]

$$a_k \mathbf{s}_k(m) \odot \phi(f) + \nu, \quad (3)$$

where a_k is a complex amplitude parameter that takes into account propagation effects and scattering, \odot denotes element-wise multiplication, ϕ is a Doppler phase vector, f is the normalized Doppler frequency, and ν is a vector of random noise and interference. The Doppler phase vector is a Vandermonde vector defined as

$$\phi(f) = [1 \quad e^{-j2\pi f} \quad \dots \quad e^{-j2\pi(L-1)f}], \quad (4)$$

where j is the imaginary unit. Additionally, let

$$\mathbf{u}_k(m, f) = \mathbf{s}_k(m) \odot \phi(f) \quad (5)$$

in order to simplify the notation.

For receiving the signal in the Doppler bin with a frequency f_b , the filter design minimizing the interference and noise power at the filter output can be written as an optimization problem [20]

$$\min_{\mathbf{w}} \mathbf{w}^H \mathbf{R}_\nu \mathbf{w} \quad (6a)$$

$$\text{s.t. } \mathbf{w}^H \mathbf{u}_k(0, f_b) = 1, \quad (6b)$$

where \mathbf{R}_ν is the interference plus noise covariance matrix. The solution to this problem,

$$\mathbf{w} = \frac{\mathbf{R}_\nu^{-1} \mathbf{u}(0, f_b)}{\mathbf{u}^H(0, f_b) \mathbf{R}_\nu^{-1} \mathbf{u}(0, f_b)}, \quad (7)$$

is the well-known MVDR beamformer [21], [22]. However, this design has the drawback that the cross-correlation and autocorrelation sidelobes cannot be controlled so that tolerable levels could be guaranteed. Therefore, additional constraints are required leading to an improved formulation for the filter design problem.

The peak sidelobe and the peak cross-correlation are defined for the k th waveform as

$$\text{PSL}_k = \max_{f,m} |\mathbf{w}^H \mathbf{u}_k(m, f)|^2, \quad |f - f_b| \geq \delta_{0m} f_w \quad (8)$$

$$\text{PCC}_k = \max_{f,i,m} |\mathbf{w}^H \mathbf{u}_i(m, f)|^2, \quad i \neq k, \quad (9)$$

where δ_{ij} is the Kronecker delta, f_w is the half-width of the main lobe in frequency, $m = -L + 1, \dots, L - 1$, and $f \in [-\frac{1}{2}, \frac{1}{2}]$ due to the sampling theorem and aliasing. The PSL and the PCC are convex functions in \mathbf{w} .

Using a mismatched filter causes a decrease in the SNR of the filter output, so it might also be necessary to control the SNR loss of the filter. The SNR loss is defined as the ratio of the matched filter SNR

$$\frac{|\mathbf{u}^H(0, f_b) \mathbf{u}(0, f_b)|^2}{\mathbf{u}^H(0, f_b) (\sigma_n^2 \mathbf{I}) \mathbf{u}(0, f_b)} = \frac{\|\mathbf{s}_k(0)\|^4}{\sigma_n^2 \|\mathbf{s}_k(0)\|^2} = \frac{1}{\sigma_n^2} \quad (10)$$

and the mismatched filter SNR

$$\frac{|\mathbf{w}^H \mathbf{u}(0, f_b)|^2}{\mathbf{w}^H (\sigma_n^2 \mathbf{I}) \mathbf{w}} = \frac{1}{\sigma_n^2 \|\mathbf{w}\|^2}, \quad (11)$$

where σ_n^2 is the noise power and (2) and (6b) were used. Constraining the SNR loss to be less than γ on linear scale, we obtain a constraint equation

$$\|\mathbf{w}\|^2 \leq \gamma. \quad (12)$$

Mismatched filters with controlled PSL, PCC, and SNR loss minimizing the output interference plus noise power can be designed by solving a constrained optimization problem

$$\min \mathbf{w}^H \mathbf{R}_\nu \mathbf{w} \quad (13a)$$

$$\text{s.t. } \max_f |\mathbf{w}^H \mathbf{u}_k(m, f)|^2 \leq \alpha, \quad |f - f_b| \geq \delta_{0m} f_w \quad (13b)$$

$$\max_f |\mathbf{w}^H \mathbf{u}_i(m, f)|^2 \leq \beta, \quad i \neq k \quad (13c)$$

$$\mathbf{w}^H \mathbf{w} \leq \gamma, \quad (13d)$$

$$\mathbf{w}^H \mathbf{u}(0, f_b) = 1, \quad (13e)$$

where α and β are the maximum allowed PSL and PCC, respectively, and γ is the constraint on the SNR loss. The constants α , β , and γ are all user-defined design parameters. Equation (13e) is needed to maintain the unit gain to the waveform of interest at zero delay. The feasibility of the problem depends on the chosen values of α , β , and γ .

The filter design for waveforms with negligible Doppler can also be done using (13) with the exception that the normalized Doppler f is zero. In this case, the optimization problem is a convex QCP. Such filter can be used with fast-time coding, for example. However, if the Doppler frequency is significant, such filter will have high sidelobes, and consequently, worse performance compared to the filter design taking the Doppler shift into account.

In the noise-only case, it is obvious that minimizing $\mathbf{w}^H \mathbf{R}_\nu \mathbf{w}$ is tantamount to minimizing the SNR loss. In such cases, it is sensible to minimize α and β instead of the output noise power.

Since the objective function and all the constraints in the problem (13) are convex, the problem itself is convex [23]. However, given that the normalized Doppler frequency f is continuous and can take any value on the interval from $-\frac{1}{2}$ to $\frac{1}{2}$, we cannot solve the filter design problem as an ordinary quadratically constrained program, as infinite number of constraints would be required to satisfy (13b) and (13c). This type of constraints can be readily converted into positive-semidefinite matrix constraints using the sum-of-squares representation [15] summarized in Section III-A.

B. Signal Cancellation

Although the waveform in the returned signal is known, the Doppler shift due to target velocity is not. If an estimated covariance matrix that contains the signal of interest is used for the interference suppression, it is possible that signal cancellation occurs. We will show that the signal loss is limited by the SNR loss constraint (12). It is also possible to restrict the signal loss further within the main lobe.

We define the signal cancellation within the Doppler bin as the ratio of the matched filter gain and the mismatched filter gain. If the maximum allowed signal cancellation is ϵ in linear scale, the signal loss constraint is given by

$$\frac{|\mathbf{u}^H(0, f_b) \mathbf{u}_k(0, f)|^2}{|\mathbf{w}^H \mathbf{u}_k(0, f)|^2} \leq \epsilon. \quad (14)$$

This constraint is unfortunately nonconvex. An alternative method to limit the signal loss is constraining the magnitude squared of the difference of the filter responses such that

$$\|[\mathbf{u}_k(0, f_b) - \mathbf{w}]^H \mathbf{u}_k(0, f)\|^2 \leq \zeta^2. \quad (15)$$

The value of ζ can be set so that the signal loss is no more than ϵ . This will place additional constraint on the phase of the mismatched filter response. However, due to the unit-gain constraint enforced for both the filters, the responses are similar also in phase near the main lobe.

Fig.1 illustrates how ζ is chosen. The filter responses are denoted by $a = \mathbf{u}^H(0, f_b) \mathbf{u}_k(0, f)$ and $b = \mathbf{w}^H \mathbf{u}_k(0, f)$ for the matched and the mismatched filter, respectively. For the signal loss to be ϵ at most, b has to be outside the solid circle, which has a radius of $\epsilon^{-1/2}|a|$ based on (14). It is easily seen that we have to have $|a| - \zeta \geq \epsilon^{-1/2}|a|$, which yields

$$\zeta = (1 - \epsilon^{-1/2}) |\mathbf{u}^H(0, f_b) \mathbf{u}_k(0, f)| \quad (16)$$

as the largest allowed ζ .

The magnitude squared of the difference of the filter responses is in fact intrinsically constrained by the SNR loss constraint (12). We can see this by writing the mismatched filter coefficients as $\mathbf{w} = \mathbf{u}(0, f_b) + \mathbf{q}$, where $\mathbf{q}^H \mathbf{u}(0, f_b) = 0$. Due to the SNR loss constraint,

$$\|\mathbf{q}\|^2 = \|\mathbf{w}\|^2 - \|\mathbf{s}_k(0)\|^2 \leq \gamma - 1. \quad (17)$$

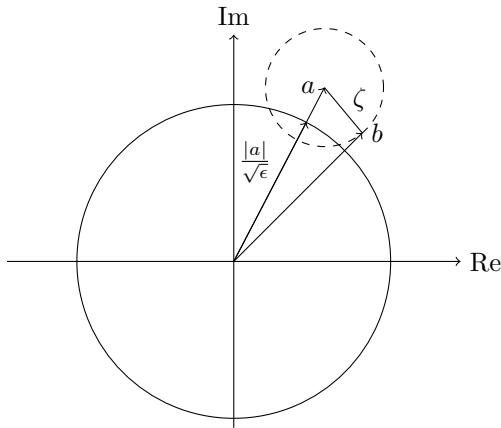


Fig. 1. Constraining the signal loss. For the signal loss to be less than ϵ , the filter response b needs to be outside the solid circle. This is achieved by constraining b to be inside the dashed circle and setting the radius ζ so that the dashed circle lies outside of the solid circle.

Thus,

$$\begin{aligned} |[\mathbf{u}_k(0, f_b) - \mathbf{w}]^H \mathbf{u}_k(0, f)|^2 &= |\mathbf{q}^H \mathbf{u}_k(0, f)|^2 \\ &\leq \|\mathbf{q}\|^2 \|\mathbf{s}_k(0) \odot \phi(f)\|^2 \quad (18) \\ &\leq \gamma - 1, \end{aligned}$$

where Cauchy-Schwarz inequality was used. This means that the radius of the dashed circle in Fig.1 is less than $\sqrt{\gamma - 1}$ for any Doppler frequency f . If it is necessary to have smaller signal loss for the frequencies near the main lobe, the convex constraint (15) can be used.

III. SEMIDEFINITE RELAXATION

In this section, we reformulate the mismatched filter optimization using the properties of a polynomial constraints. The resulting optimization problem is then solved using semidefinite relaxation. In case the rank of the SDR solution is higher than one so that solution cannot be directly factorized into the filter coefficients, a randomization method for generating approximate solutions is also proposed.

A. Polynomial Constraints

Many signal processing problems and filter design problems in particular can be formulated as constrained optimization problems. Many of the encountered constraints can be recast as nonnegative polynomial constraints [15]. Such constraints can be further converted into equality constraints and linear matrix inequalities using the sum-of-squares representation.

The basic idea is following: Suppose that we need to confirm whether or not a polynomial p of degree $2d$ in real variables $\mathbf{y} = [y_1 \ y_2 \ \dots]^T$ is nonnegative. The sufficient condition for this is to write p as a sum of squares,

$$p(\mathbf{y}) = \sum_i q_i^2(\mathbf{y}) \quad (19)$$

Alternatively, if the vector $\boldsymbol{\mu}$ contains all the monomials of degree less or equal to d in the variables y_i , we can write the polynomial as

$$p(\mathbf{y}) = \boldsymbol{\mu}^T \mathbf{X} \boldsymbol{\mu}. \quad (20)$$

If the matrix \mathbf{X} is positive-semidefinite, then the polynomial p is necessarily nonnegative. For more details, the reader is referred to [24], [15], and the references therein.

In the mismatched filter design problem, we are particularly interested in real-valued, trigonometric polynomials of the form

$$p(\omega) = z_0 + 2\text{Re}\left\{ \sum_{n=1}^{L-1} z_n e^{-j\omega n} \right\}. \quad (21)$$

This type of polynomials allows us to use Theorems 1 and 2 of [15]. First, define the vector \mathbf{z} using the coefficients in (21) as

$$\mathbf{z} = [z_0 \ z_1 \ \dots \ z_{L-1}]^T. \quad (22)$$

Also, define the matrix \mathbf{F}_L as a matrix containing the L first columns of a full $M \times M$ DFT matrix, i.e.

$$\mathbf{F}_L = \begin{bmatrix} 1 & 1 & \dots & 1 \\ 1 & e^{-j2\pi/M} & \dots & e^{-j2\pi(L-1)/M} \\ \vdots & \vdots & \ddots & \vdots \\ 1 & e^{-j2\pi(M-1)/M} & \dots & e^{-j2\pi(M-1)(L-1)/M} \end{bmatrix}, \quad (23)$$

$L \leq M$. Similarly, define a matrix \mathbf{F}_{L-1} to consist of $L-1$ first columns of the $M \times M$ DFT matrix.

Theorem 1: A trigonometric polynomial of the form given in (21) is nonnegative on the interval $[0, 2\pi]$ if and only if there is an $L \times L$ positive-semidefinite matrix \mathbf{X} such that

$$\mathbf{z} = \mathbf{F}_L^H \text{diag}(\mathbf{F}_L \mathbf{X} \mathbf{F}_L^H), \quad (24)$$

where $M \geq 2N + 1$ and $\text{diag}(\mathbf{F}_L \mathbf{X} \mathbf{F}_L^H)$ denotes the vector consisting of the elements on the main diagonal of the matrix $\mathbf{F}_L \mathbf{X} \mathbf{F}_L^H$.

Theorem 2: A trigonometric polynomial of the form given in (21) is nonnegative on the interval $[\omega_0 - \Delta, \omega_0 + \Delta]$ if and only if there are an $L \times L$ positive-semidefinite matrix \mathbf{X} and an $(L-1) \times (L-1)$ positive-semidefinite matrix \mathbf{Y} such that

$$\mathbf{z} = \mathbf{F}_L^H [\text{diag}(\mathbf{F}_L \mathbf{X} \mathbf{F}_L^H) + \mathbf{c} \odot \text{diag}(\mathbf{F}_{L-1} \mathbf{Y} \mathbf{F}_{L-1}^H)], \quad (25)$$

where the n th element of the vector \mathbf{c} is

$$c_n = \cos(2\pi(n-1)/M - \omega_0) - \cos(\Delta), \quad (26)$$

$n = 1 \dots M$.

The proofs of these theorems are provided in [15, p. 946].

B. Semidefinite Formulation

The basic formulation of mismatched filter optimization problem was given in (13). In order to obtain a solvable problem, we need to convert the constraints (13b) and (13c) into trigonometric polynomials that are then required to be

nonnegative. We first note that

$$\begin{aligned}
 & |\mathbf{w}^H \mathbf{u}_i(m, f)|^2 \\
 &= |[\mathbf{w} \odot \mathbf{s}_i^*(m)]^H \phi(f)|^2 \\
 &= \phi^H(f) [\mathbf{w} \odot \mathbf{s}_i^*(m)] [\mathbf{w} \odot \mathbf{s}_i^*(m)]^H \phi(f) \\
 &= \phi^H(f) [\mathbf{w} \mathbf{w}^H \odot \mathbf{s}_i^*(m) \mathbf{s}_i^T(m)] \phi(f) \\
 &= \sum_{k=1}^L \sum_{n=1}^L e^{j2\pi f(k-1)} (\mathbf{w} \mathbf{w}^H \odot \mathbf{s}_i^*(m) \mathbf{s}_i^T(m))_{kn} e^{-j2\pi f(n-1)} \\
 &= \sum_{k=1}^L \sum_{n=1}^L e^{j2\pi f(k-n)} w_k w_n^* (\mathbf{s}_i(m))_k^* (\mathbf{s}_i(m))_n, \\
 &= \sum_{n=1}^L w_n w_n^* (\mathbf{s}_i(m))_n^* (\mathbf{s}_i(m))_n \\
 &\quad + 2\text{Re} \left\{ \sum_{n=1}^L e^{-j2\pi f n} \sum_{k=n+1}^L w_{k-n} w_k^* (\mathbf{s}_i(m))_{k-n}^* (\mathbf{s}_i(m))_k \right\}, \tag{27}
 \end{aligned}$$

where the last equality results from collecting the terms with equal value of $k - n$. This is a real-valued trigonometric polynomial of the form (21), where the n th coefficient of the polynomial is given by

$$z_n = \sum_{k=n+1}^L w_{k-n} w_k^* (\mathbf{s}_i(m))_{k-n}^* (\mathbf{s}_i(m))_k \tag{28}$$

and $\omega = 2\pi f$.

The constraint polynomials for filter design are

$$\alpha - |\mathbf{w}^H \mathbf{u}_k(m, f)|^2 \geq 0, \tag{29a}$$

$$\beta - |\mathbf{w}^H \mathbf{u}_i(m, f)|^2 \geq 0. \tag{29b}$$

For each waveform \mathbf{s}_i and delay m , we need a coefficient vector $\mathbf{z}_{i,m}$ and a PSD matrix $\mathbf{X}_{i,m}$ for forming the sum-of-squares presentation of the constraint.

Equation (28) is a quadratic equality constraint, which is nonconvex. In order to obtain a convex problem, we apply semidefinite relaxation (SDR) and replace $w_{k+n} w_n^*$ in (28) by $(\mathbf{W})_{k+n,n}$, where \mathbf{W} is an $L \times L$ positive-semidefinite matrix. The j th element of the coefficient vector $\mathbf{z}_{i,m}$ is defined as

$$(\mathbf{z}_{i,m})_j = \delta_{0j} \alpha - \sum_{n=1}^{L-j} (\mathbf{W})_{j+n,n} (\mathbf{s}_i(m))_{j+n}^* (\mathbf{s}_i(m))_n \tag{30}$$

for $i = k$ and as

$$(\mathbf{z}_{i,m})_j = \delta_{0j} \beta - \sum_{n=1}^{L-j} (\mathbf{W})_{j+n,n} (\mathbf{s}_i(m))_{j+n}^* (\mathbf{s}_i(m))_n \tag{31}$$

for $i \neq k$.

Theorem 1 in [15] can now be directly applied to express the constraint (29b) as

$$\mathbf{z}_{i,m} = \mathbf{F}_L^H \text{diag}(\mathbf{F}_L \mathbf{X}_{i,m} \mathbf{F}_L^H), \mathbf{X}_{i,m} \succeq 0, \tag{32}$$

for the waveform number $i \neq k$ and delay m , where $\mathbf{X}_{i,m} \succeq 0$ means that $\mathbf{X}_{i,m}$ is positive-semidefinite.

Next, a similar formulation is needed for the PSL constraint (29a). For nonzero delays, this can be done the same way as

for the PCC constraint in (32). We apply Theorem 2 to deal with the zero delay and the main lobe. Let f_w be the Doppler half-width of the main lobe. Defining the elements of vector \mathbf{c} as

$$c_n = \cos(2\pi(n-1)/M - \pi - 2\pi f_b) - \cos(\pi - 2\pi f_w), \tag{33}$$

the PSL constraint for $m = 0$ can be written as

$$\begin{aligned}
 \mathbf{z}_{k,0} &= \mathbf{F}_L^H [\text{diag}(\mathbf{F}_L \mathbf{X}_{k,0} \mathbf{F}_L^H) + \mathbf{c} \odot \text{diag}(\mathbf{F}_{L-1} \mathbf{Y}_0 \mathbf{F}_{L-1}^H)], \\
 \mathbf{X}_{k,0} &\succeq 0, \mathbf{Y}_0 \succeq 0, \tag{34}
 \end{aligned}$$

where \mathbf{Y}_0 is an $(L-1) \times (L-1)$ PSD matrix. Consequently, the semidefinite relaxation of the filter design problem can be written as

$$\min \text{tr}(\mathbf{W} \mathbf{R}_{\mathbf{v}}) \tag{35a}$$

$$\begin{aligned}
 \text{s.t } \mathbf{z}_{k,0} &= \mathbf{F}_L^H [\text{diag}(\mathbf{F}_L \mathbf{X}_{k,0} \mathbf{F}_L^H) \\
 &\quad + \mathbf{c} \odot \text{diag}(\mathbf{F}_{L-1} \mathbf{Y}_0 \mathbf{F}_{L-1}^H)] \tag{35b}
 \end{aligned}$$

$$\mathbf{z}_{i,m} = \mathbf{F}_L^H \text{diag}(\mathbf{F}_L \mathbf{X}_{i,m} \mathbf{F}_L^H), (i, m) \neq (k, 0) \tag{35c}$$

$$\text{tr}(\mathbf{W}) \leq \gamma \tag{35d}$$

$$\text{tr}\{\mathbf{W} \mathbf{u}(0, f_b) \mathbf{u}^H(0, f_b)\} = 1 \tag{35e}$$

$$\mathbf{W} \succeq 0, \mathbf{X}_{i,m} \succeq 0, \mathbf{Y}_0 \succeq 0, \tag{35f}$$

where the notation $(i, m) \neq (k, 0)$ means that both $i = k$ and $m = 0$ cannot hold simultaneously. The problem in (35) is a convex optimization problem so the global optimum can be found efficiently [23].

If the main lobe signal loss has to be constrained, (15) has to be converted into a polynomial form. The required polynomial constraint is

$$\zeta^2 - |[\mathbf{u}_k(0, f_b) - \mathbf{w}]^H \mathbf{s}_k(0) \odot \phi(f)|^2 \geq 0 \tag{36}$$

on the interval $[f_b - f_B, f_b + f_B]$, where the size of the Doppler bin is $2f_B$. Similar to the PSL constraint, we define a coefficient vector \mathbf{z}_B with the elements

$$(\mathbf{z}_B)_j = \delta_{0j} \zeta^2 - \sum_{n=1}^{L-j} (\mathbf{Q})_{j+n,n} (\mathbf{s}_i(m))_{j+n}^* (\mathbf{s}_i(m))_n, \tag{37}$$

where

$$\begin{aligned}
 \mathbf{Q} &= \mathbf{W} - \mathbf{u}(0, f_b) \mathbf{w}^H - \mathbf{w} \mathbf{u}^H(0, f_b) \\
 &\quad + \mathbf{u}(0, f_b) \mathbf{u}^H(0, f_b). \tag{38}
 \end{aligned}$$

The additional constraints for the SDR problem (35) are then

$$\begin{aligned}
 \mathbf{z}_B &= \mathbf{F}_L^H [\text{diag}(\mathbf{F}_L \mathbf{X}_B \mathbf{F}_L^H) \\
 &\quad + \mathbf{c}_B \odot \text{diag}(\mathbf{F}_{L-1} \mathbf{Y}_B \mathbf{F}_{L-1}^H)] \tag{39a}
 \end{aligned}$$

$$\mathbf{w}^H \mathbf{u}(0, f_b) = 1 \tag{39b}$$

$$\mathbf{W} - \mathbf{w} \mathbf{w}^H \succeq 0, \mathbf{X}_B \succeq 0, \mathbf{Y}_B \succeq 0, \tag{39c}$$

with the elements of \mathbf{c}_B given by

$$(c_B)_n = \cos(2\pi(n-1)/M - 2\pi f_b) - \cos(2\pi f_B). \tag{40}$$

An alternative to (36) is to directly constrain the signal loss such that

$$|\mathbf{w}^H \mathbf{u}_k(0, f)|^2 \geq \epsilon \tag{41}$$

for the Doppler frequencies in the Doppler bin. This non-convex constraint can be converted into a polynomial constraint in the same fashion as (29a) and (29b) and becomes convex after the relaxation.

The proposed mismatched filter design can also be used for mitigation of strong, spatially distinct clutter that is present in low-angle land clutter, for example [25]. The clutter in a particular bin is equal to

$$\mathbf{r}(m, f_b) = \sum_{i,n} \tilde{\sigma}_{i,n}^{1/2} \mathbf{u}_i(\tilde{m}_{i,n} - m, \tilde{f}_{i,n} - f_b), \quad (42)$$

where $\tilde{\sigma}_{i,n}$ is the power, $\tilde{m}_{i,n}$ is the delay, and $\tilde{f}_{i,n}$ is the Doppler frequency of clutter source n for waveform i (the waveform-dependency of the quantities is for a radar system with distributed transmitters). Assuming that the clutter is strong, estimating its power, delay, and Doppler is trivial. The clutter can then be mitigated by minimizing an objective function

$$\text{tr}(\mathbf{W}\mathbf{R}_v) + \text{tr}\{\mathbf{W}\mathbf{r}(m, f_b)\mathbf{r}^H(m, f_b)\} \quad (43)$$

corresponding the total interference and clutter power in the particular Doppler bin in place of (35a). The disadvantage of this approach is that each range–Doppler bin needs its own filters.

C. Randomization

The solution of the optimization problem (35) is a positive-semidefinite matrix, denoted by \mathbf{W}_o . If the rank of \mathbf{W}_o is equal to one, the filter coefficients may be found by using factorization $\mathbf{W}_o = \mathbf{w}_o\mathbf{w}_o^H$. In this case, the filter coefficient vector \mathbf{w}_o is the globally optimal solution to the nonrelaxed problem [17]. Given that the problem using the sum-of-squares representation is just an alternative formulation of the original problem in (13), the factorization \mathbf{w}_o of the rank-one matrix is also the globally optimal solution of the original problem (13).

It is plausible that the solution of the SDR problem has a rank that is higher than one, especially if the nonconvex constraint (41) is used. For this reason, it is necessary to have a method for generating a suitable filter even in the case that the SDR solution cannot be simply factorized into the filter coefficients.

A randomization method can be used to obtain the filter coefficients from a SDR solution with a rank larger than one. Randomization is done by generating random solution candidates $\tilde{\mathbf{w}}$ from the complex normal distribution [17]

$$\tilde{\mathbf{w}} \sim \mathcal{CN}(\mathbf{0}, \mathbf{W}_o). \quad (44)$$

However, the probability for the randomized candidates to satisfy the unit gain constraint (13e) is zero. Therefore, we project $\tilde{\mathbf{w}}$ to be orthogonal to $\mathbf{u}_k(0, f_b)$ using a projection matrix \mathbf{P} ,

$$\mathbf{P} = \mathbf{I} - \mathbf{u}(0, f_b)\mathbf{u}^H(0, f_b), \quad (45)$$

so that $\mathbf{u}^H(0, f_b)\mathbf{P}\tilde{\mathbf{w}} = 0$. The SNR loss constraint (13d) can be satisfied by scaling $\mathbf{P}\tilde{\mathbf{w}}$ so that its norm does not exceed

$\sqrt{\gamma - 1}$. Thus, a filter coefficient vector

$$\mathbf{w} = \mathbf{u}(0, f_b) + \min\left(1, \frac{\sqrt{\gamma - 1}}{\|\mathbf{P}\tilde{\mathbf{w}}\|}\right)\mathbf{P}\tilde{\mathbf{w}} \quad (46)$$

will satisfy both (13d) and (13e). There is no simple way to guarantee that the randomized solution would satisfy the PSL constraint (13b) or the PCC constraint (13c). However, if the interior of the set that satisfies (13b) and (13c) is non-empty, then clearly the probability that the randomized solution is feasible is larger than zero. Numerous randomized filter coefficient vectors can be generated easily and the one that provides the lowest interference power at the output with suitable PSL and PCC levels can be chosen as the final filter.

If the main lobe signal loss constraint (39) is used, the randomization procedure is the same, only the distribution $\mathcal{CN}(\mathbf{w}_o, \mathbf{W}_o - \mathbf{w}_o\mathbf{w}_o^H)$ is used for drawing the candidates.

IV. APPROXIMATE FILTER DESIGN

For a filter with L coefficients and a waveform with N symbols, there are $N + L - 1$ delay values to consider, each of which requires an $L \times L$ positive-semidefinite matrix in the SDR filter optimization problem (35). The total number of $L \times L$ PSD matrices needed to control the PSL and PCC levels is therefore the $N + L - 1$ times the number of waveforms (an additional $(L - 1) \times (L - 1)$ PSD matrix is needed for the zero delay), resulting in a high computational complexity. Instead of using the sum-of-squares representation to satisfy the trigonometric polynomial constraints, we can reduce the computational complexity by discretizing the Doppler frequency similar to FIR filter design approach in [26].

Given a grid of Doppler frequencies f_j , $j = 1, 2, \dots$, the approximate filter design can be written as an optimization problem

$$\min \mathbf{w}^H \mathbf{R} \mathbf{w} \quad (47a)$$

$$\text{s.t. } |\mathbf{w}^H \mathbf{u}_k(m, f_j)|^2 \leq \alpha, \quad |f_j - f_b| \geq \delta_{0m} f_w \quad (47b)$$

$$|\mathbf{w}^H \mathbf{u}_i(m, f_j)|^2 \leq \beta, \quad i \neq k \quad (47c)$$

$$\mathbf{w}^H \mathbf{w} \leq \gamma, \quad (47d)$$

$$\mathbf{w}^H \mathbf{u}(0, f_b) = 1. \quad (47e)$$

This is a convex quadratically constrained problem from which the filter coefficients \mathbf{w} are obtained directly. For Doppler values between the frequencies f_j , (47b) and (47c) do not necessarily hold anymore. However, $|\mathbf{w}^H \mathbf{u}_i(m, f)|^2$ varies smoothly as a function of the Doppler frequency f , so by using an increasingly denser set of points, the amount by which the maximum PSL and PCC values exceed α or β can be made arbitrarily small.

The number of constraints in (47) depends linearly on the number of the Doppler grid points. As the number of iterations required for an interior-point method to converge is independent on the number of constraints [23], the computational complexity of solving this approximate problem grows only linearly with the number of grid points when everything else is kept constant.

The approximate mismatched filter design in interference-free case can be written as

$$\min \max(\alpha, \beta) \quad (48a)$$

$$\text{s.t } |\mathbf{w}^H \mathbf{u}_k(m, f_j)|^2 \leq \alpha, \quad |f_j - f_b| \geq \delta_{0m} f_w \quad (48b)$$

$$|\mathbf{w}^H \mathbf{u}_i(m, f_j)|^2 \leq \beta, \quad i \neq k \quad (48c)$$

$$\mathbf{w}^H \mathbf{w} \leq \gamma, \quad (48d)$$

$$\mathbf{w}^H \mathbf{u}(0, f_b) = 1. \quad (48e)$$

It should be noted that in this case, there is no need to calculate the mismatched filter for each Doppler bin, but the same filter can be shifted in frequency for each bin.

The constraint for the main lobe signal loss (15) can be discretized as precisely the same way as the PSL and the PCC constraints.

If no Doppler frequency points other than $f_i = 0$ are considered, the optimization problem becomes essentially the same as the one presented in [12].

V. PSL AND PCC LEVEL SELECTION

So far, the PSL and the PCC level have been assumed to be given. In practice, one needs to select these parameters depending on the situation. Both high interference power and high PSL and PCC levels reduce the performance of the radar receiver, so it is important to select the design parameters as well as possible.

Having good interference rejection and achieving low PSL and PCC levels are competing design goals, and the adequate trade-off between these depends on the task at hand as well as the interference and the propagation environments. Assume, for example, that the power of one of the received waveforms is significantly higher compared to the other waveforms. If the allowed PCC level of the filter is equal for all the waveforms, the strong waveform will cause added interference. However, this interference can be reduced simply by using mismatched filters with decreased cross-correlation level for the powerful waveform.

As a further example of sidelobe level selection, we consider the detection of a Swerling I type target in Gaussian noise with a constant false alarm rate. It is well-known that the uniformly most powerful test of detecting this type of target compares the filter output power to a threshold τ , which depends on the interference and noise power as well as the chosen constraint on the probability of false alarm p_f ,

$$p_f = \text{Prob}(|\mathbf{w}^H \boldsymbol{\nu}|^2 \geq \tau). \quad (49)$$

Since the noise plus interference $\boldsymbol{\nu}$ is assumed to be zero-mean complex Gaussian process with the covariance matrix \mathbf{R}_ν ,

$$\mathbf{w}^H \boldsymbol{\nu} \sim \mathcal{CN}(0, \mathbf{w}^H \mathbf{R}_\nu \mathbf{w}), \quad (50)$$

and the threshold value is given by

$$\tau = \mathbf{w}^H \mathbf{R}_\nu \mathbf{w} F_{\chi_2^2}^{-1}(1 - p_f) = -\mathbf{w}^H \mathbf{R}_\nu \mathbf{w} \, 2 \log p_f, \quad (51)$$

where $F_{\chi_2^2}^{-1}$ is the inverse cumulative distribution function of central chi-square random variable with two degrees of freedom.

The sidelobe level parameter α can be chosen so that the probability of incorrectly detecting the target range or Doppler due to a sidelobe is equal to p_e . This requirement can be written as

$$\text{Prob}(|\alpha a + \mathbf{w}^H \boldsymbol{\nu}|^2 \geq \tau) = p_e, \quad (52)$$

where a is the amplitude of the scattered signal. According to the Swerling I model [27], a is a zero-mean complex normal random variable. Due to the unit gain constraint of the mismatched filter, the variance of a is equal to the signal power σ_s^2 at the filter output. A condition identical to (52) is thus

$$\begin{aligned} F_{\chi_2^2}((\mathbf{w}^H \mathbf{R}_\nu \mathbf{w} + \alpha \sigma_s^2)^{-1} \tau) &= 1 - p_e \\ \Rightarrow \frac{\mathbf{w}^H \mathbf{R}_\nu \mathbf{w} F_{\chi_2^2}^{-1}(1 - p_f)}{\mathbf{w}^H \mathbf{R}_\nu \mathbf{w} + \alpha \sigma_s^2} &= F_{\chi_2^2}^{-1}(1 - p_e) \end{aligned}$$

resulting in

$$\alpha \frac{\sigma_s^2}{\mathbf{w}^H \mathbf{R}_\nu \mathbf{w}} = \frac{\log p_f}{\log p_e} - 1, \quad (53)$$

which shows the relationship between the sidelobe level α , the signal to interference plus noise ratio (SINR) that is equal to $\sigma_s^2 / (\mathbf{w}^H \mathbf{R}_\nu \mathbf{w})$, the probability of false alarm p_f and the probability of error in detection p_e . The target values for the sidelobe level α and the output interference power can be determined using this equation and the filter design problem can then be solved in order to see if a feasible filter can be found.

VI. NUMERICAL EXAMPLES

Numerical examples of the proposed mismatched filter design are presented in this section. First, we will compare the matched filter to the mismatched filters obtained by solving the SDR problem and the approximate QCP. We then give an example of the interference mitigation with the mismatched filter and demonstrate how an estimate of the interference plus noise covariance matrix can be successfully used.

A. Minimum PSL and PCC

Given the difficulty of the waveform optimization for MIMO radar use, it is sensible to use mismatched filters in the receivers to improve the ambiguity properties of the waveforms. As an example, we optimize the mismatched filters for a set of four QPSK waveforms with 40 symbols in each. Only white noise is assumed to be present with no interference. The mismatched filters were designed to have as low PSL and PCC as possible while the SNR loss was constrained to 1 dB.

Different MIMO radar waveform design methods to minimize PSL and PCC have been proposed before. For example, [5] used adaptive annealing to find four polyphase codes of length 40 with zero-Doppler PSL of -14.80 dB and PCC of -13.47 dB. A genetic algorithm was used in [6] to obtain four polyphase codes of length 40 with PSL of -16.02 dB and PCC of -12.75 dB. However, the Doppler effect was not taken into account in the optimization of these waveform sets. Thus, the PSL and PCC levels of these sequences are much higher when a nonzero Doppler shifts are allowed, namely

−8.00 dB and −6.71 dB for the former and −7.97 dB and −6.87 dB for the latter.

Using the proposed mismatched filter design, it is possible to improve the PSL and PCC levels at the receiver. First, we compare the proposed design to a filter design that ignores the Doppler frequency. The filters were designed to receive the first sequence of [5]. When the Doppler frequency is ignored, the filter design problem is as in (13), but the normalized Doppler frequency f is identically zero. The resulting the sidelobes and cross-correlation are equal to −16.62 dB along the zero-cut of the ambiguity function, but the overall PSL and PCC of the entire ambiguity functions are equal to −6.46 and −6.91 dB, respectively. For the proposed design in which the normalized Doppler can take values on $[-\frac{1}{2}, \frac{1}{2}]$, the overall PSL and PCC are both equal to −9.49 dB, so the resulting filter is significantly better for scenarios with a significant Doppler shift.

Next, the optimal SDR filters and the approximate QCP filters in (48) with 256 Doppler grid points were calculated for the entire four-waveform set. The PSL and PCC levels of the SDR mismatched filters were −9.12 dB for the set of [5] and −9.24 dB for the waveforms in [6], so the PSL and PCC levels were significantly improved compared to the matched filters.

Fig. 2 shows the maximum of the cross-ambiguity function of the waveform number 2 of the set in [5] with the matched and the mismatched filters. The maximum is taken over the normalized Doppler frequency in Fig. 2(a) and over the delay in Fig. 2(b), so

$$\max_f |\mathbf{w}^H [\mathbf{s}_2(m) \odot \phi(f)]|^2 \quad (54)$$

is plotted in (a) and

$$\max_m |\mathbf{w}^H [\mathbf{s}_2(m) \odot \phi(f)]|^2 \quad (55)$$

in (b). Compared to the matched filter, both the SDR and the QCP mismatched filters improve the PSL level considerably, while the difference between the mismatched filter designs is small.

Fig. 3 shows the maximum cross-ambiguity for the waveform number four and the filters intended for waveform number two. Also in this case, the mismatched filters have a significantly lower PCC than the matched filter, and the difference between the SDR and QCP mismatched filters is very small.

In order to compare the matched and mismatched filters further, we created sets of four QPSK sequences of 40 symbols similar to the waveforms in [5] and [6]. In the first set, the symbols were chosen randomly. The PSL of this set is −7.70 dB and PCC is −6.09 dB. The second set was optimized with simulated annealing with 250 random initializations resulting in a PSL of −8.52 dB and a PCC of −8.18 dB. The third set of sequences was created so that it would have high cross-correlation. This was achieved by taking a single random sequence and then changing 20% of the symbols randomly in each sequence. The PSL and PCC of this set were −7.58 dB and −2.65 dB, respectively.

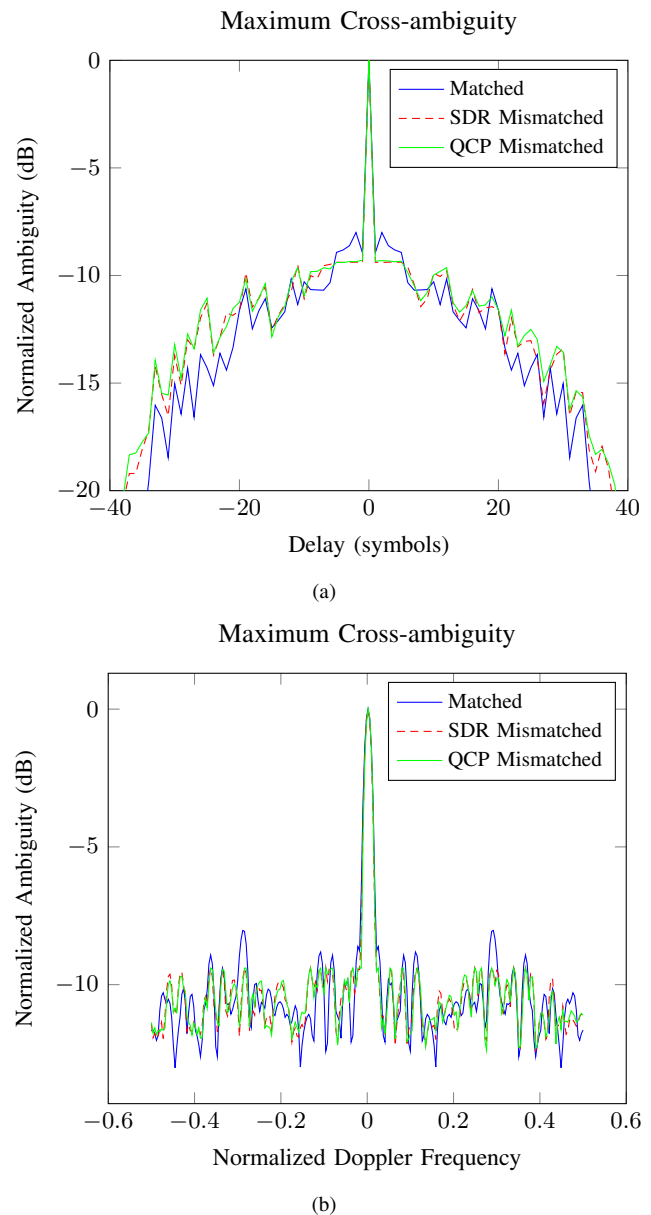


Fig. 2. Maximum cross-ambiguity of the waveform two of [5] and the receiver filters over (a) the Doppler frequency and (b) the delay. Lower sidelobes are achieved with the mismatched filters. The difference between the SDR and the approximate QCP filters is small.

The results of the mismatched filter optimization for all the waveform sets are summarized in Table I. We can make following observations from the results. Naturally, the PSL and PCC of the mismatched filters for the optimized waveforms are the lowest, but the difference to the random waveforms is small, much smaller than for the matched filters. Furthermore, by using the mismatched filters, the PCC of the high cross-correlation waveform set that would otherwise be unusable can be reduced to a manageable level of −7.14 dB. Therefore, it is possible to compensate the deficiencies of the waveforms using mismatched filters.

The maximum cross-ambiguity function of the high-cross-correlation waveform set and the matched filter as well as the SDR-optimized mismatched filter are shown in Fig. 4.

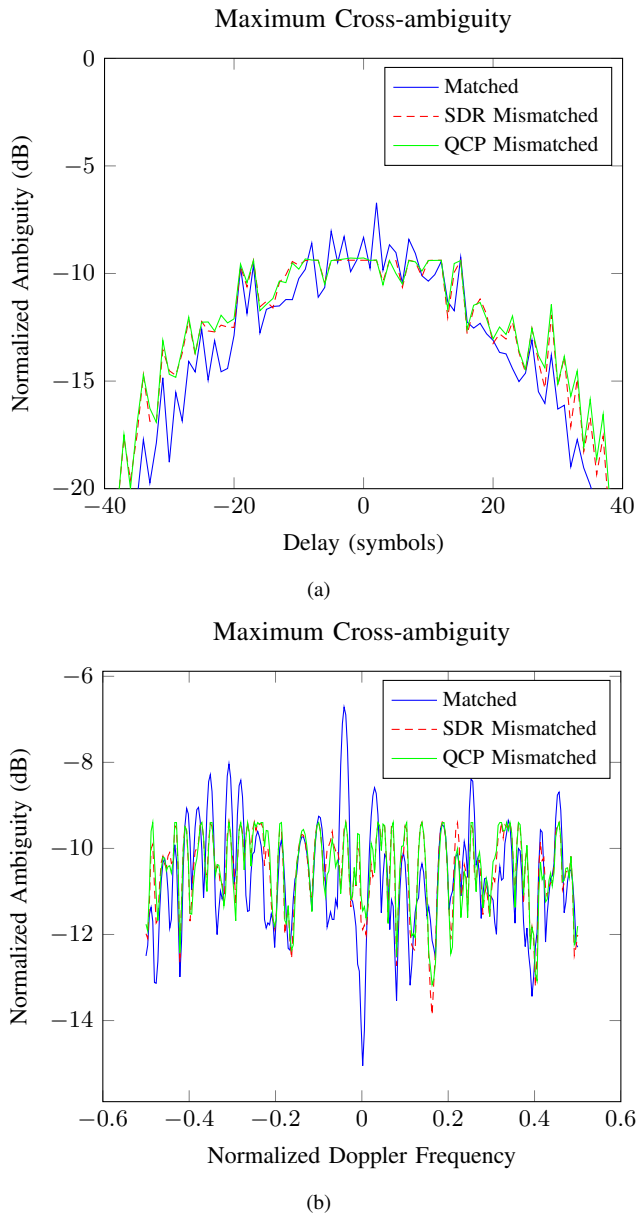


Fig. 3. Maximum cross-ambiguity of the waveform number four in [5] and the receiver filters for waveform two over (a) the Doppler frequency and (b) the delay. Considerably lower peak cross-correlation is achieved with the mismatched filters. Again, the difference between the SDR and the approximate QCP filters is small.

Due to the similarity of the waveforms in this set, there is a peak in cross-correlation at zero Doppler shift for the matched filter. The mismatched filter is able to minimize these cross-correlation peaks resulting in a drastic decrease of the PCC level.

B. Interference Mitigation

Next, we show an example of interference mitigation using the proposed mismatched filter design. The waveforms in this case are Oppermann polyphase codes [28]. Some of these codes have desirable correlation properties, but the drawback is the large number of different symbols needed. The remarkable benefit, however, is the ability to obtain numerous sequences

TABLE I
PSL AND PCC OF MATCHED AND MISMATCHED FILTERS FOR SELECTED CODE SETS

Code set	Matched		Mismatched QCP		Mismatched SDR	
	PSL	PCC	PSL	PCC	PSL	PCC
Hai Deng [5]	-8.00	-6.71	-9.04	-9.00	-9.12	-9.12
Bo Liu et al. [6]	-7.97	-6.87	-8.90	-9.11	-9.24	-9.24
Random	-7.70	-6.09	-8.96	-8.92	-9.07	-9.07
Optimized	-8.52	-8.18	-8.81	-9.33	-9.48	-9.48
High cross-corr.	-7.58	-2.65	-7.12	-7.08	-7.14	-7.14

Comparison of PSL and PCC levels of matched and mismatched filters. The PSL and PCC can be reduced with mismatched filtering at the cost of SNR loss that was constrained to 1 dB in this case. The differences between the globally optimal SDR and the approximate QCP filters are small.

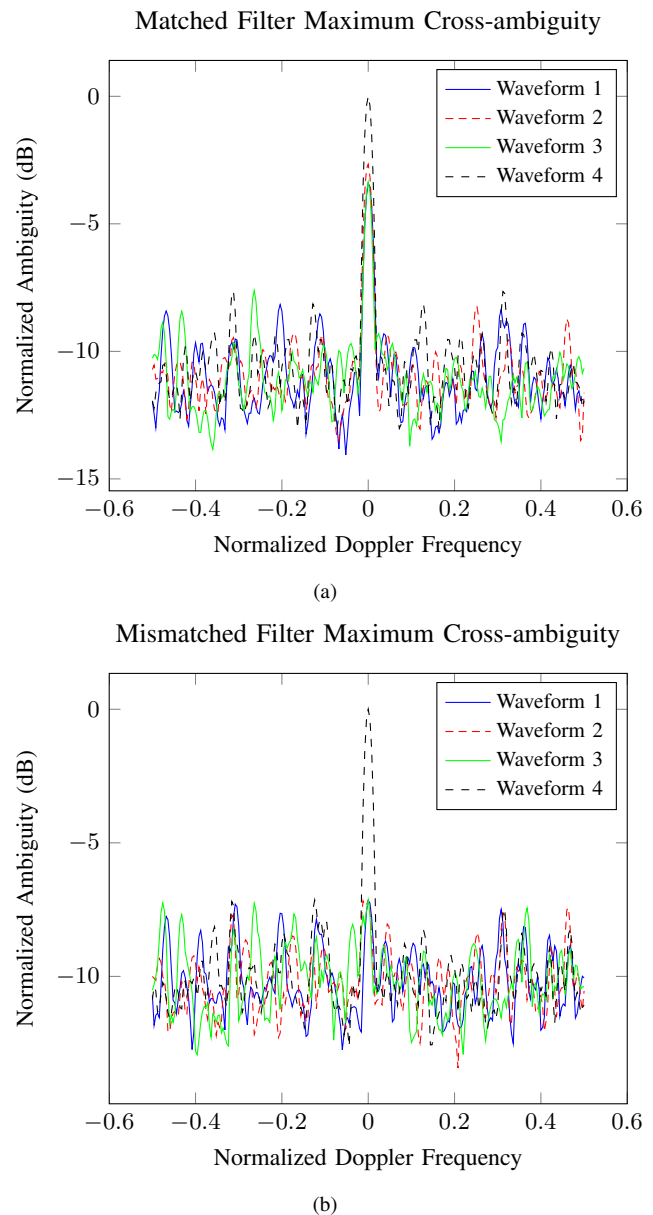


Fig. 4. Maximum cross-ambiguity of the waveform set with high cross-correlation for (a) matched filter and (b) the mismatched filter for the fourth waveform. The mismatched filter does not have the cross-correlation peaks at zero Doppler that the matched filter has.

of varying length with low peak autocorrelation sidelobe (PSL) and peak cross-correlation (PCC) by tuning just a few parameters.

The Oppermann codes are given by [28]

$$s_i(m) = (-1)^{im} \exp\left(\frac{j\pi(i^k m^p + m^n)}{N}\right), \quad (56)$$

where j is the imaginary unit, N is the sequence length, i is the sequence number, m is the symbol index, and k, n , as well as p are parameters. The transmitted waveforms in this example were three Oppermann codes with the parameter values $N = 61$, $i = 1, 2, 3$, $k = 2$, $n = 3$, and $p = 3$. These codes have PCC of -9.13 dB and PSL of -12.29 dB assuming nonzero Doppler shift. The second code corresponding to $i = 2$ was the waveform of interest that the filters were designed to receive.

In order to compare the interference mitigation performance, we define the SINR gain as the ratio of the SINR of the particular filter \mathbf{w} to the SINR of the matched filter. This SINR gain is given by

$$G_{\text{SINR}} = \frac{|\mathbf{w}^H \mathbf{u}_k(0, f_b)|^2 / \mathbf{w}^H \mathbf{R}_\nu \mathbf{w}}{\frac{|\mathbf{u}_k^H(0, f_b) \mathbf{u}_k(0, f_b)|^2 / \mathbf{u}_k^H(0, f_b) \mathbf{R}_\nu \mathbf{u}_k(0, f_b)}{\mathbf{u}_k^H(0, f_b) \mathbf{R}_\nu \mathbf{u}_k(0, f_b)}} \quad (57)$$

where the assumption $\|\mathbf{s}_k(0)\| = 1$ and the constraint $\mathbf{w}^H \mathbf{s}_k(0) = 1$ were used.

In the following numerical examples, the interference is a Gaussian random process with an autocorrelation function

$$r(m) = \sigma_I^2 \frac{(L-m)(L-m+1)(2L+m+1)}{L(L+1)(2L+1)} e^{j2\pi m/7}, \quad (58)$$

which corresponds to a narrow peak slightly off the center frequency. The interference power is denoted by σ_I^2 . The receiver noise was i.i.d. white Gaussian noise and the interference to noise ratio (INR) was 20 dB.

The proposed mismatched filter design was compared to the matched filter, the MVDR filter given by (7), and the minimum PSL and PCC filter with an SNR loss constraint. For the matched filter, the PSL was -12.89 dB and the PCC -9.13 dB. Being the baseline, the SNR loss and SINR gain are both zero dB for the matched filter. The MVDR filter minimizes the output interference power and its SINR gain is 9.44 dB. However, the effective interference mitigation comes at the cost of increased PSL at -9.08 dB and PCC at -7.72 dB.

A mismatched filter with 121 coefficients minimizing the PSL and PCC levels was designed using the QCP design of (48). A grid of 256 equally spaced points were used for Doppler frequency and the SNR loss was constrained to 1 dB. The resulting filter had a PSL of -11.56 dB and PCC of -11.30 dB; however, the SINR gain was -1.92 dB implying that the interference is amplified, which is highly undesirable.

On the other hand, if the mismatched filter is designed according to (47) to minimize the output interference power with the same SNR loss and grid points and α and β equal to 0.075 (approximately -11.25 dB), an SINR gain of 8.45 dB is achieved. The PSL and PCC that were -11.08 dB and

TABLE II
MISMATCHED FILTER OPTIMIZATION FOR OPPERMANN CODES

Filter Type	PSL	PCC	SNR Loss	SINR Gain
Matched	-12.89	-9.13	0.00	0.00
MVDR	-9.08	-7.72	1.54	9.44
Min PSL&PCC	-11.56	-11.30	1.00	-1.92
Proposed	-11.08	-10.87	0.78	8.45
Proposed, $\hat{\mathbf{R}}$ Avg. ^a	-11.25	-11.25	1.00	7.78

Comparison of PSL and PCC levels as well as interference suppression of different filter types. The proposed filter can provide good interference mitigation with low PSL and PCC, even when the covariance matrix estimate is used. ^a Averaged over 100 trials using a covariance matrix estimate

-10.78 dB¹, respectively, were only slightly higher compared to the design minimizing only the PSL and the PCC.

The mismatched filter optimization in (47) requires that the interference plus noise covariance matrix is known. This is typically not the case in practice, so the covariance matrix would have to be estimated. In case of low number of samples available for estimation, regularized estimators can be used [18], [19].

The covariance matrix estimation was simulated by creating 121 samples of the received signal containing the waveform of interest with a SNR of 5 dB and the interfering signal as well as noise. The filter optimization was performed in one hundred independent trials using the estimated covariance matrix $\hat{\mathbf{R}}$ and the results were averaged and then converted into dB. The average SINR gain was 7.78 dB. Despite using the covariance matrix estimate, the interference could still be attenuated effectively without significant changes in the PSL and PCC levels. The filter optimization results are summarized in Table II.

The minimum PSL and PCC level and interference suppression performance are naturally competing design goals, but filters that achieve a good trade-off between these two can be obtained with the proposed design method. This is highlighted in Fig. 5 that displays the approximate Pareto frontier of the mismatched filters for the described setup. The Pareto frontier shows the combination of the highest SINR gain and the lowest achievable PSL and PCC level, demonstrating that near either end of the curve, the SINR gain or the PSL and PCC level can be improved without significant deterioration of the other.

The lower left point in Fig. 5 corresponds to the minimum PSL and PCC design whereas the upper right point is the MVDR filter with no PSL or PCC constraints. It can be seen that near the lower end of the achievable PSL and PCC, the SINR gain can be improved significantly with only a small increase in the PSL and PCC levels. Likewise in the high SINR gain end, the PSL and PCC can be reduced by several dB with only minute decrease in the SINR gain compared to the MVDR filter.

A more practical example of the use of the mismatched filter is shown Fig.6. There are three targets located in range bins

¹PSL and PCC are higher than the design value of -11.25 dB as the peak values do not occur at the grid points.

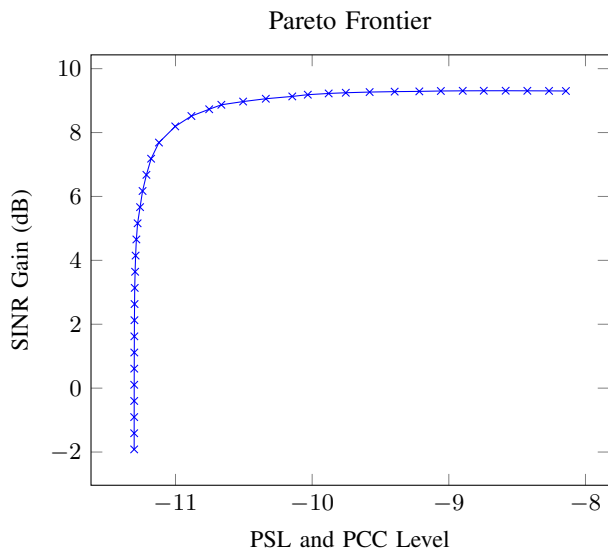


Fig. 5. Pareto frontier of the mismatched filter design showing the best achievable combinations of the SINR gain and minimum PSL and PCC. Filters with excellent trade-off between PSL and PCC level and SINR gain can be achieved along the Pareto curve.

30, 50, and 100 having normalized Doppler frequencies 0.2, -0.3 , and 0.1 , respectively. The SNR of the signal from each target is 5 dB. The interfering signal is same as previously with an INR of 20 dB.

The range–Doppler plot of the matched filter is shown in Fig.6(a). None of the targets can be seen because of the strong interference. Mismatched filter was calculated for each Doppler bin so that the PSL and PCC were at same level as with the matched filter and the interference power was minimized. In the resulting range–Doppler plot in Fig.6(b), the targets can be easily distinguished.

Another example in Fig.7 demonstrates the clutter mitigation with mismatched filters. The setup is similar to that of Fig.6, but in addition to interference, there is a strong, isolated clutter source with a normalized Doppler frequency of -0.1 and a clutter to noise ratio of 15 dB in the range bin number 70. The mismatched filter can be used to mitigate the interference, but it is difficult to detect the targets because of the high sidelobes from the clutter in Fig.7(a). When the combined clutter and interference power is minimized in each range–Doppler bin as in Fig.7(b), the targets clearly stand out.

C. Computational complexity

In Section IV, the approximate filter design was introduced to reduce the computational complexity of the mismatched filter optimization. In order to compare the computational complexity of the SDR method and the QCP approximation, we measured the CPU time required to calculate mismatched filters for waveform of differing lengths N , where the filter length L was 40. The waveforms were generated randomly. The computations were performed on a desktop with a Intel Xeon E31230 CPU running at 3.2Ghz.

The CPU time for the both methods is shown in Fig.8. The number of waveforms is equal to K , and the lines are fitted to

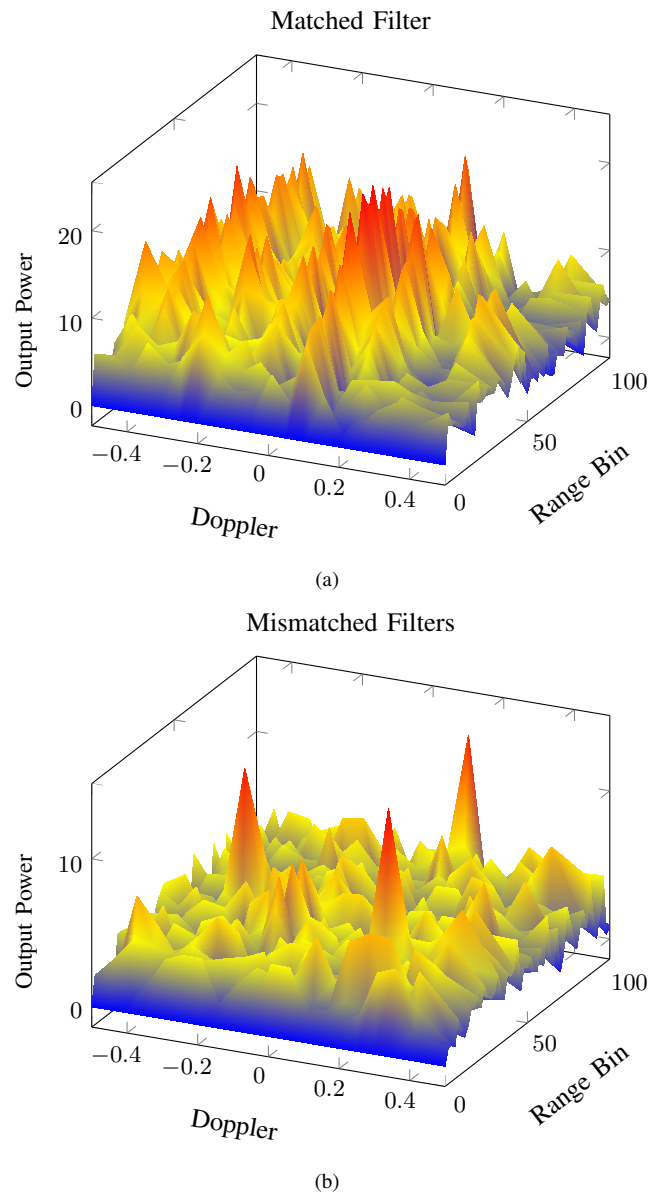


Fig. 6. Range–Doppler plots for (a) matched filter and (b) mismatched filters. The targets are buried in the interference when the matched filter is used but are clearly distinguishable with the mismatched filter.

the data in the least-squares sense for each value of K . For the QCP problem, the complexity clearly depends polynomially on the problem size, and based on the slopes of the lines, the complexity is approximately $\mathcal{O}(K(L + N)^{7/2})$. On the other hand, the SDR formulation in Fig.8(b) has much higher computational complexity.

The CPU time is intended only for illustrating the difference between the methods. In practice, the filters could be solved much faster using a dedicated solvers and parallelization.

VII. CONCLUSIONS

Mismatched filters can be used for suppressing interference while simultaneously decreasing the autocorrelation sidelobe and peak cross-correlation levels of the waveforms in a MIMO radar system. We proposed a method for designing such

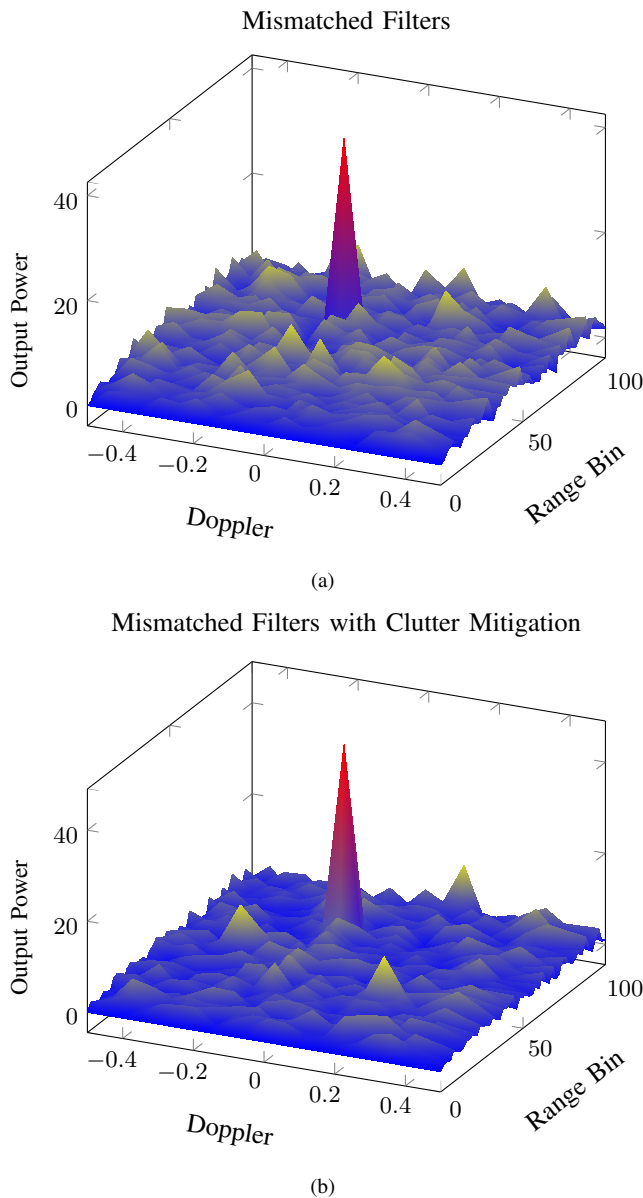


Fig. 7. Range–Doppler plots for (a) mismatched filters with interference mitigation and (b) mismatched filters with combined interference and clutter mitigation. Without the clutter mitigation, it is difficult to detect the targets in (a) because of the sidelobes. With the clutter mitigation in (b), targets are clearly visible.

filters by minimizing the filter output interference power while constraining the peak autocorrelation sidelobe and peak cross-correlation to a tolerable level for all Doppler frequencies. The proposed design is formulated as an SDP by employing sum-of-squares representation of nonnegative polynomials and semidefinite relaxation. Due to the relatively high computational complexity of this approach, we proposed an alternative optimization method that discretizes the Doppler frequency to form a convex quadratically constrained problem. Only a minor performance loss is experienced with this approximate method.

In the presence of a nonwhite interfering signal, mismatched filters not taking the interference into account might unintentionally amplify the interference. The proposed design minimizes

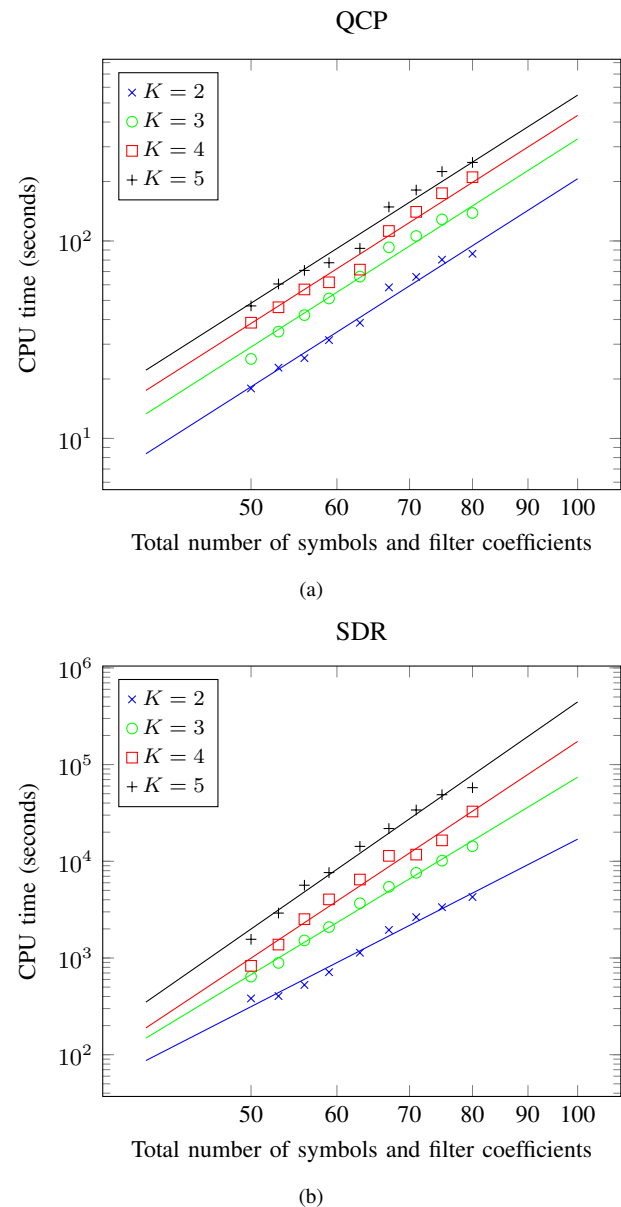


Fig. 8. The CPU time needed for optimizing the mismatched filter using (a) QCP approximation or (b) SDR formulation. The number of waveforms is K . The QCP approximation is computationally much less complex than the SDR formulation of the problem.

ing the output interference power produces much better performance in such scenarios with only a minimal increase in the peak sidelobe and cross-correlation levels. A very good trade-off can be achieved between the interference attenuation and minimum PSL and PCC levels. Furthermore, the interference can be effectively attenuated using an interference plus noise covariance matrix estimate even when there is a component of the signal of interest present in the observed data.

REFERENCES

- [1] A.M. Haimovich, R.S. Blum, and L.J. Cimini, “MIMO radar with widely separated antennas,” *IEEE Signal Processing Magazine*, vol. 25, no. 1, pp. 116–129, 2008.
- [2] Jian Li and Petre Stoica, “MIMO radar with colocated antennas,” *IEEE Signal Processing Magazine*, vol. 24, no. 5, pp. 106–114, Sept 2007.

[3] Jian Li and Petre Stoica, Eds., *MIMO Radar Signal Processing*, John Wiley & Sons, 2009.

[4] B.M. Keel and T.H. Heath, "A comprehensive review of quasi-orthogonal waveforms," in *IEEE Radar Conference*, 2007, pp. 122–127.

[5] Hai Deng, "Polyphase code design for orthogonal netted radar systems," *IEEE Transactions on Signal Processing*, vol. 52, no. 11, pp. 3126–3135, Nov 2004.

[6] Bo Liu, Zishu He, Jiankui Zeng, and Benyong Liu, "Polyphase orthogonal code design for MIMO radar systems," in *International Conference on Radar*, Oct 2006, pp. 1–4.

[7] Dali Liu, Yuntao Liu, and Huizhi Cai, "Orthogonal polyphase code sets design for MIMO radar using tabu search," in *IEEE International Conference on Intelligent Control, Automatic Detection and High-End Equipment*, 2012, pp. 123–127.

[8] H.A. Khan, Yangyang Zhang, C. Ji, C.J. Stevens, D.J. Edwards, and D. O'Brien, "Optimizing polyphase sequences for orthogonal netted radar," *IEEE Signal Processing Letters*, vol. 13, no. 10, pp. 589–592, Oct 2006.

[9] Martin H. Ackroyd and F. Ghani, "Optimum mismatched filters for sidelobe suppression," *IEEE Transactions on Aerospace and Electronic Systems*, vol. AES-9, no. 2, pp. 214–218, 1973.

[10] Petre Stoica, Jian Li, and Ming Xue, "On binary probing signals and instrumental variables receivers for radar," *IEEE Transactions on Information Theory*, vol. 54, no. 8, pp. 3820–3825, Aug 2008.

[11] A. De Maio, M. Piezzo, S. Iommelli, and A. Farina, "Design of pareto-optimal radar receive filters," *International Journal of Electronics and Telecommunications*, vol. 57, no. 4, pp. 477–481, 2011.

[12] Liangbing Hu, Hongwei Liu, Da zheng Feng, Bo Jiu, Xu Wang, and Shunjun Wu, "Optimal mismatched filter bank design for MIMO radar via convex optimization," in *International Waveform Diversity and Design Conference (WDD)*, aug 2010, pp. 126–131.

[13] T. Aittomäki and V. Koivunen, "MIMO radar filterbank design for interference mitigation," in *IEEE International Conference on Acoustics, Speech and Signal Processing (ICASSP)*, May 2014, pp. 5297–5301.

[14] Petre Stoica, Jian Li, and Ming Xue, "Transmit codes and receive filters for radar," *IEEE Signal Processing Magazine*, vol. 25, no. 6, pp. 94–109, November 2008.

[15] T. Roh and L. Vandenberghe, "Discrete transforms, semidefinite programming, and sum-of-squares representations of nonnegative polynomials," *SIAM Journal on Optimization*, vol. 16, no. 4, pp. 939–964, 2006.

[16] Antonio De Maio, Yongwei Huang, M. Piezzo, Shuzhong Zhang, and Alfonso Farina, "Design of optimized radar codes with a peak to average power ratio constraint," *IEEE Transactions on Signal Processing*, vol. 59, no. 6, pp. 2683–2697, June 2011.

[17] Zhi-Quan Luo, Wing-Kin Ma, A.M.-C. So, Yinyu Ye, and Shuzhong Zhang, "Semidefinite relaxation of quadratic optimization problems," *IEEE Signal Processing Magazine*, vol. 27, no. 3, pp. 20–34, May 2010.

[18] Ying Sun, P. Babu, and D.P. Palomar, "Regularized tyler's scatter estimator: Existence, uniqueness, and algorithms," *IEEE Transactions on Signal Processing*, vol. 62, no. 19, pp. 5143–5156, Oct 2014.

[19] E. Ollila and D.E. Tyler, "Regularized m-estimators of scatter matrix," *IEEE Transactions on Signal Processing*, vol. 62, no. 22, pp. 6059–6070, Nov 2014.

[20] B.D. Van Veen and K.M. Buckley, "Beamforming: A versatile approach to spatial filtering," *IEEE ASSP Magazine*, vol. 5, no. 2, pp. 4–24, Feb 1988.

[21] Simon Haykin, *Adaptive Filter Theory*, Prentice Hall, fourth edition, 2002.

[22] Dimitris G. Manolakis, Vinay K. Ingle, and Stephen M. Kogon, *Statistical and adaptive signal processing : spectral estimation, signal modeling, adaptive filtering and array processing*, McGraw-Hill, 2000.

[23] Stephen Boyd and Lieven Vandenberghe, *Convex Optimization*, Cambridge University Press, 2004.

[24] Pablo A. Parrilo, "Semidefinite programming relaxations for semialgebraic problems," *Mathematical Programming*, vol. 96, no. 2, pp. 293–320, 2003.

[25] J. Barrie Billingsley, *Low-Angle Radar Land Clutter*, William Andrew Publishing, 2002.

[26] Shao-Po Wu, S. Boyd, and L. Vandenberghe, "FIR filter design via semidefinite programming and spectral factorization," in *Proceedings of the 35th IEEE Conference on Decision and Control*, 1996, vol. 1, pp. 271–276.

[27] Merrill I. Skolnik, Ed., *Radar Handbook*, McGraw-Hill, second edition, 1990.

[28] I. Oppermann, "Orthogonal complex-valued spreading sequences with a wide range of correlation properties," *IEEE Transactions on Communications*, vol. 45, no. 11, pp. 1379–1380, nov 1997.



Tuomas Aittomäki received a M.Sc. (Tech) degree with distinction in applied physics in 2009 from the Helsinki University of Technology, Finland. He is currently pursuing a D.Sc. degree at School of Electrical Engineering of Aalto University. His research interests include antenna arrays, radar signal processing, and MIMO radars.



Visa Koivunen (F11) received his D.Sc. (EE) degree with honors from the University of Oulu, Dept. of Electrical Engineering. He received the primus doctor award among the doctoral graduates in years 1989–1994. He is a member of Eta Kappa Nu. From 1992 to 1995 he was a visiting researcher at the University of Pennsylvania, Philadelphia, USA. Since 1999 he has been a full Professor of Signal Processing at Aalto University (formerly known as Helsinki Univ of Technology), Finland. He received the Academy professor position (distinguished professor nominated by the Academy of Finland). Years 2003–2006 he was also adjunct full professor at the University of Pennsylvania, Philadelphia, USA. He has also been a part-time Visiting Fellow at Nokia Research Center (2006–2012). He has spent multiple mini-sabbaticals and two full sabbaticals at Princeton University.

Dr. Koivunen's research interests include statistical, communications, sensor array and multichannel signal processing. He has published more than 370 papers in international scientific conferences and journals and holds 6 patents. He co-authored the papers receiving the best paper award in IEEE PIMRC 2005, EUSIPCO2006, EUCAP (European Conference on Antennas and Propagation) 2006 and COCORA 2012. He has been awarded the IEEE Signal Processing Society best paper award for the year 2007 (with J. Eriksson). He served as an associate editor for IEEE Signal Processing Letters and IEEE TR on Signal Processing. He has served as co-editor for two IEEE JSTSP special issues. He was a member of editorial board for IEEE Signal Processing Magazine. He has been a member of the IEEE Signal Processing Society technical committees SPCOM-TC and SAM-TC. He was the general chair of the IEEE SPAWC 2007 conference in Helsinki, Finland June 2007 and Technical Program Chair for the IEEE SPAWC 2015. He was awarded the 2015 EURASIP (European Association for Signal Processing) Technical Achievement Award for fundamental contributions to statistical signal processing and its applications in wireless communications, radar and related fields. He is a member of the IEEE Fourier Award committee and IEEE SPS Distinguished Lecturer for 2015–2016.